Mitochondrial dysfunction, through impaired autophagy, mediates ER stress, deregulates lipid metabolism, and drives pancreatitis

Gyorgy Biczo,[1,2,3]* Eszter T. Vegh,[1,2,3]* Natalia Shalbueva,[1,2] Olga A. Mareninova,[1,2] Jason Elperin,[1,2] Ethan Lotshaw,[1,2] Sophie Gretler,[1,2] Aurelia Lugea,[5] Sudarshan R. Malla[1,2], David Dawson,[1] Piotr Ruchala,[1] Julian Whitelegge,[1] Samuel W. French,[6] Li Wen,[7] Sohail Z. Husain,[7] Fred S. Gorelick,[8] Peter Hegyi,[9,10] Zoltan Rakonczay Jr,[3,4] Ilya Gukovsky,[1,2] Anna S. Gukovskaya.[1,2]

Supplementary Materials

Materials and Methods

Experimental pancreatitis. Arg-AP was induced in Sprague-Dawley rats by 2 hourly i.p. injections of 3 g/kg Arg; and in wild-type C57BL/6 (wt), CypD$^{-/-}$ (Refs. [1, 2]), transgenic GFP-LC3 (Ref. [3]) and compound GFP-LC3;CypD$^{-/-}$ mice, by 3 hourly i.p. injections of 3.3 g/kg Arg. CER-AP was induced by 7 hourly injections of 50 µg/kg cerulein. Control mice received saline injections. Animals were killed at indicated times (2 to 72 h after the first injection of Arg or 7 h after the first injection of CER).

TLCS-AP was induced, as described in Ref.[4], by retrograde infusion of TLCS dissolved in saline into the distal common bile and pancreatic duct. Briefly, mice were anesthetized with a ketamine (120 mg/kg)/xylazine (12 mg/kg) mixture (Butler Schein, Chicago, IL), and ventral incision was made to reveal the abdominal cavity. The duodenum was flipped to reveal its distal side and held in place by ligatures. The bile duct was identified, and a 30-gauge needle was inserted through the antimesenteric aspect of the duodenum to cannulate the biliopancreatic duct. TLCS was infused at 10 µl/min for 5 min using a P33 perfusion pump (Harvard Apparatus, Holliston, MA). The exterior wound was closed using 7-mm wound clips, and a single injection of buprenorphine (0.075 mg/kg) was given immediately after the surgery. Saline-infused mice served as controls. Animals were allowed to recover on a heating pad for 90 min after the procedure, and were euthanized 6 or 24 h after induction. Tissue was collected, and mitochondria isolated, from the head of the pancreas, as in bile-acid infusion AP models the injury is predominantly localized to pancreatic head.[5]

CDE-AP was induced in young (14–15 g) female mice fed either CDE or control diet.[6] Fresh aliquots of the diets were provided every 12 hours, and the food intake was measured. Mice were sacrificed 24 or 48 hours after initiation of the diet.

CypD deficient mice were generated by targeted disruption of the *Ppif* gene[7] and provided to us by Dr. Michael A. Forte (Oregon Health and Sciences University). The genetic background

of these mice is C57Bl/6J; and since 2010, CypD null mice were back-crossed for >10 generations into a C57BL/6J genetic background. We have reported data obtained on these mice.[1, 2]

In experiments aimed to restore efficient autophagy, 2 g/kg trehalose (Sigma-Aldrich) dissolved in phosphate-buffered saline (PBS) was given in mice by daily i.p. injections for 12 days followed by induction of Arg-AP or CER-AP. Mice were killed 24 h after the first Arg injection or 7 h after the first CER injection.

The experimental protocols were approved by the animal research committee of the Veterans Affairs Greater Los Angeles Healthcare System, in accordance with NIH Guidelines.

Human pancreas specimens. Tissue specimens of human normal pancreas and pancreatitis were provided de-identified by the UCLA Department of Pathology Pancreas Tissue Bank (D.D.), according to a protocol approved by the UCLA Institutional Review Board. Normal pancreas and pancreatitis tissue specimens, provided as formalin-fixed paraffin embedded samples, were primarily procured from surgical resection specimens where malignant disease was absent. All normal pancreas tissues were obtained from remnant portions of Whipple and distal pancreatectomy specimens from patients who underwent resection for causes that included duodenal adenoma, low grade mucinous cystic neoplasm or well-differentiated pancreatic neuroendocrine tumor. In all instances, the pathologic lesion was well-circumscribed and the normal pancreatic tissue was taken from an area of pancreas parenchyma at least 2 cm distant from the pathologic lesion. All H&E sections were carefully evaluated (D.D.) for the presence of acinar compartment and to confirm, in particular, that the procured normal tissue had no histological abnormalities (i.e., pancreatitis, necrosis, PanIN's, etc).

Isolation of pancreatic acinar cells. Acinar cells were isolated from control or Arg-treated mice using a standard collagenase digestion procedure.[1, 2, 8]

Isolation of mitochondria and measurements of $\Delta\Psi m$. Mitochondria were isolated from rat or mouse pancreas and liver in a Ca^{2+}-free medium in the presence of 1 mM EGTA as described.[1, 2, 8] In all preparations of mitochondria from normal pancreas (isolated and assayed in

the presence of 1 mM EGTA) the value of respiratory control ratio measured in the presence of succinate was greater than 3.0 (Ref. [8]). Measurements of oxygen consumption demonstrated coupled respiration of pancreatic mitochondria isolated in the presence of 1 mM EGTA. ADP produced state III respiration in a standard manner. Mitochondria also developed uncoupled respiration after the addition of CCCP, comparable with a state-III rate. We measured the mitochondrial membrane potential ($\Delta\Psi m$) using a tetraphenyl phosphonium (TPP^+) electrode, as described;[1, 2, 8] and the respiration, using a Clark-type electrode, in mitochondria suspension (1 mg/ml protein) in a buffer containing (mM) 250 sucrose, 22 KCl, 22 triethanolamine (pH 7.4), 3 $MgCl_2$, 5 KH_2PO_4, 1 EGTA, supplemented with 0.5% BSA and 10 mM glutamate and 2 mM malate as the respiratory substrate. Variations in basal $\Delta\Psi m$ between mitochondria preparations from normal mouse (as well as rat) pancreas did not exceed 3%. In studies of $\Delta\Psi m$ dependence on Ca^{2+}, Ca^{2+}/EGTA buffers (Molecular Probes, Eugene, OR) were used to maintain free Ca^{2+} concentrations at “zero”, 1.0, 2.0, and 5.0 μM. The Ca^{2+}/EGTA buffer was supplemented with 10 mM glutamate and 2 mM malate used as the respiratory substrate. An increase in $\Delta\Psi m$ results in TPP^+ uptake by mitochondria and, correspondingly, a decrease in external TPP^+ concentration measured with TPP^+ electrode. The mitochondrial uncouplers, such as FCCP (carbonyl cyanide p-trifluoromethoxyphenylhydrazone) or dinitrophenol (DNP), were added at the end of each experiment to cancel $\Delta\Psi m$ and thus determine the “zero $\Delta\Psi m$” level.

To further assess the quality of our mitochondria preparations, we measured by immunoblot the levels of several mitochondrial markers in these preparations, such as the mitochondrial outer membrane proteins TOM40 and TOM20 (widely used to assess the number and integrity of mitochondria), and the mitochondria resident proteins VDAC, CypD, and COX IV, as illustrated in Figure S6*D*.

Incubation of mouse pancreatic mitochondria (for up to ~25 min observation) with 100 nM CCK-8 or with 20-40 mM Arg had no effect on ΔΨm. (Longer incubations are not feasible because isolated mitochondria gradually lose their functions if incubated for > ~25 min.)

Preparation of submitochondrial particles and measurements of F-ATP synthase activity. These were performed as in Ref. [9]. Briefly, mitochondria were sonicated in the presence of 15 mM $MgCl_2$ and 1 mM ATP followed by 10-min centrifugation at 43,000 x g; the supernatant was collected and further centrifuged for 30 min at 100,000 x g. Submitochondrial particles (the pellet) were suspended in a buffer containing 250 mM sucrose, 10 mM Tris/ MOPS (pH7.4), 5 mM succinate, 20 µM EGTA and 2 µM rotenone, at a protein concentration of 0.8 mg/ml. F-ATP synthase activity was measured spectrophotometrically (at 340 nm) by the reduction of $NADP^+$ via the hexokinase and glucose-6-phosphate dehydrogenase reactions. The assay mixture contained 1 mM ADP, 10 mM potassium phosphate (pH 7.5), 10 mM succinate, 50 mM HEPES, 1 mM glucose, 1 mM $NADP^+$, 2 mM $MgCl_2$, 2 mg/ml fatty acid-free BSA, 200 mM sucrose, 20 IU hexokinase, and 7.0 IU glucose-6-phosphate dehydrogenase. The reaction was initiated by addition of the submitochondrial particles. The rate of NADPH production was followed for 3 min, then 5 µg/ml oligomycin was added and the reaction was followed for another 2 min. The rate of NADPH production sensitive to oligomycin was taken as F-ATP synthase activity.

ΔΨm and [Ca^{2+}]i measurements in isolated pancreatic acinar cells. Upon isolation, the cells were re-suspended in a buffer containing (mM) 140 NaCl, 4.7 KCl, 1.1 $MgCl_2$, 1.0 $CaCl_2$, 10 D-glucose, 10 HEPES (adjusted to pH 7.2 by NaOH), 10 pyruvate and 1 glutamine, and loaded for 20 min at 37 °C with 1 µM ΔΨm-sensitive fluorescent dye TMRM or with 2 µM Ca^{2+}-sensitive dye Fura-2AM. Measurements of ΔΨm and [Ca^{2+}]i were performed at 37 °C in temperature-controlled cuvette of the Shimadzu RF-1501 spectrofluorometer (Shimadzu, Kyoto, Japan) as described.[2] The TMRM fluorescence intensity was recorded at 543 nm (excitation) and 570 nm (emission), and the results were presented in arbitrary units. At the TMRM concentrations applied, its fluorescence is quenched when the dye is accumulated by mitochondria.[10] Thus, an increase

in ΔΨm manifests itself by a decrease in TMRM fluorescence intensity. For quantitative analysis of ΔΨm changes, the difference between TMRM fluorescence in cells before and after addition of the mitochondrial uncoupler FCCP (carbonyl cyanide p-trifluoromethoxy-phenylhydrazone) was considered as 100% ΔΨm.

Changes in $[Ca^{2+}]i$ were measured as the ratio of Fura-2 fluorescence emitted at 510 nm upon 340 or 380 nm excitation. Digitonin was added at the end of each experiment to obtain the fluorescence intensity of Fura-2 when saturated with Ca^{2+}.

Trypsin activity was measured in homogenates of pancreatic tissue by a fluorogenic assay using Boc-Gln-Ala-Arg-AMC as a substrate, as previously described.[11, 12]

ATP levels in pancreatic tissue samples were measured using ATP determination kit (Molecular Probes, Eugene, OR).

Serum amylase and lipase levels were measured in a Hitachi 707 analyzer (Antech Diagnostics, Irvine, CA).

Immunoprecipitation. CypD and F-ATP synthase were immunoprecipitated from mitochondrial protein lysates using, correspondingly, anti-CypD antibody (PA3-022, Thermo Fisher Scientific, Rockford, IL) or F-ATP synthase Immunocapture Kit (ab109715, Abcam, Cambridge, MA.[13] The same antibodies were used for IB detection of these proteins. Immunoprecipitated proteins were collected using Catch and Release® kit (Millipore, Charlottesville, VA) according to the manufacturer's protocol. In direct IB, the F-ATP synthase antibody recognizes prominent bands at ~25 kDa and 55 kDa; the latter is not shown in Figure 2 because in the immunoprecipitate it is masked by IgG band.

IB analysis was performed on homogenates of pancreatic or liver tissue, isolated mitochondria, or immunoprecipitates as described.[11] Proteins were separated by SDS-PAGE, transferred to nitrocellulose membrane, and probed with antibodies against GRP78, CHOP, LC3, p62/SQSTM1, p65/RelA, phospho-p65, ERK1/2 (Cell Signaling, Danvers, MA); DLP1, OPA1 (BD Bioscience, Franklin Lakes, NJ); MFN1 (Novus Biological, Littleton, CO); and Fis1 (Biovision, San

Francisco, CA). ERK1/2 and GAPDH served as loading control. Blots were developed for visualization using enhanced chemiluminescence detection kit, and band intensities were quantified by densitometry using the FluorChem HD2 imaging system (Alpha Innotech, Santa Clara, CA)

IF and IHC analyses were performed on paraffin-embedded pancreatic tissue sections after xylene deparaffinization, graded ethanol re-hydration, and heat-induced antigen retrieval (with 10 mM citrate, pH 6.0). Nonspecific binding was blocked with 5% rabbit or goat serum. For IF analysis, tissue sections were stained with primary antibodies against Tom20 (Santa Cruz), VDAC1 (Abcam), or HMGB1 (Novus Biologicals) followed by incubation with FITC- or Texas Red conjugated secondary antibodies. Nuclei were stained with DAPI. IF images were acquired in a Zeiss LSM710 confocal microscope using x63 objective. Quantitative co-localization analysis was performed on z-stack with Volocity Image Analysis software (PerkinElmer, Waltham, MA), using Manders-Costes or Pearson colocalization coefficients. For IHC, endogenous peroxidase was blocked with 3% hydrogen peroxide, followed by incubation of pancreatic tissue sections with primary antibody against MPO (DAKO, Santa Clara, CA) or F4/80 (Abcam), and visualization with streptavidin-biotin immunoenzymatic antigen detection system (Vector Laboratories, Burlingame, CA). Quantification of MPO and F4/80 immunolabeling was performed with ImageJ software.

Electron microscopy**.** For electron microscopy, the tissue (cut into 1-mm cubes) was fixed overnight at 4 °C in 2.5% glutaraldehyde, 150 mM sodium cacodylate (pH 7.4). After post-fixation in 1% OsO4 followed by uranyl acetate, the tissue was dehydrated in ethanol and embedded in epoxy resin. 100-nm-thick sections were examined in a Hitachi-600 electron microscope.

Lipidomics. The analyses were performed by the University of California San Diego (UCSD) LIPID MAPS Lipidomics Core. Measurements of total levels of phosphatidylcholine, phosphatidylethanolamine, tri- and diacylglycerols were performed by LC-MS analysis. Free fatty acids were extracted using a liquid/liquid protocol in which the nonpolar layer is collected and

dried. The extracted fatty acids were derivatized using pentaflourylbenzylbromine and analyzed by gas chromatography using an Agilent GC/MS ChemStation. Individual analytes were monitored using selective ion monitoring, analyzed by peak area, and quantified by the isotope dilution method using a deuterated internal standard and a standard curve.

Measurements of free Arg concentration were performed using LC-MS analysis.[14] Briefly, samples of pancreatic and liver tissue or isolated pancreatic and liver mitochondria were homogenized in PBS, centrifuged, and the supernatants were mixed with 3 volumes of dimethyl sulfoxide/acetonitrile mixture (1:1) containing 0.1% trifluoroacetic acid to precipitate proteins and nucleic acids. Low molecular weight components were separated by centrifugation and analyzed using Agilent 6460 Triple Quadrupole LC-MS System (Agilent Technologies, Santa Clara, CA), equipped with a TSK gel column (2.0×150 mm, 4 μm, 125 Å, MICHROM Bioresources Inc., Auburn, CA). Methyl ester of N-benzoyl-Arg was used as an internal standard. The results are expressed per mg protein.

Electrophoretic mobility shift assay (EMSA). NF-κB DNA binding activity was measured with the Odyssey Infrared EMSA Kit for the analysis of DNA-protein interactions (LI-COR Biosciences), according to manufacturer's instructions. Double stranded oligonucleotide probe containing a consensus κB binding motif (5'-AGTTGAGGGGACTTTCCCAGGC, annealed to its complementary oligonucleotide and end-labeled with infrared dye) was used in EMSA.

Measurements of necrosis, apoptosis, and vacuolization. Quantification of necrosis and acinar cell vacuolization was performed on H&E-stained pancreatic tissue samples based on morphologic criteria, as described.[11, 12] Apoptosis was measured with TUNEL assay (Promega, Madison, WI) as the percent of nuclei stained positively for fragmented DNA, quantified by using the Volocity Image Analysis software.

Statistical analysis. Data are presented as mean $\pm$ SEM. Statistical analysis was performed with Prizm5 software (GraphPad, San Diego, CA) using two-tailed Student's *t*-test. $P < .05$ was considered statistically significant.

Study approval. All experimental protocols were approved by the animal research committee of VA Greater Los Angeles Healthcare System, in accordance with NIH guidelines.

References for Supplementary Materials

1. **Mukherjee R, Mareninova OA**, Odinokova IV, et al. Mechanism of mitochondrial permeability transition pore induction and damage in the pancreas: inhibition prevents acute pancreatitis by protecting production of ATP. Gut 2016;65:1333-46.
2. Shalbueva N, Mareninova OA, Gerloff A, et al. Effects of oxidative alcohol metabolism on the mitochondrial permeability transition pore and necrosis in a mouse model of alcoholic pancreatitis. Gastroenterology 2013;144:437-446 e6.
3. Mizushima N, Yamamoto A, Matsui M, et al. In vivo analysis of autophagy in response to nutrient starvation using transgenic mice expressing a fluorescent autophagosome marker. Mol Biol Cell 2004;15:1101-11.
4. Muili KA, Wang D, Orabi AI, et al. Bile acids induce pancreatic acinar cell injury and pancreatitis by activating calcineurin. J Biol Chem 2013;288:570-80.
5. Vaquero E, Gukovsky I, Zaninovic V, et al. Localized pancreatic NF-kappaB activation and inflammatory response in taurocholate-induced pancreatitis. Am J Physiol Gastrointest Liver Physiol 2001;280:G1197-208.
6. Lu SC, Gukovsky I, Lugea A, et al. Role of S-adenosylmethionine in two experimental models of pancreatitis. FASEB J 2003;17:56-8.
7. Basso E, Fante L, Fowlkes J, et al. Properties of the permeability transition pore in mitochondria devoid of Cyclophilin D. J Biol Chem 2005;280:18558-61.
8. Odinokova IV, Sung KF, Mareninova OA, et al. Mechanisms regulating cytochrome c release in pancreatic mitochondria. Gut 2009;58:431-42.
9. Haynes V, Traaseth NJ, Elfering S, et al. Nitration of specific tyrosines in FoF1 ATP synthase and activity loss in aging. Am J Physiol Endocrinol Metab 2010;298:E978-87.

10. Voronina SG, Barrow SL, Gerasimenko OV, et al. Effects of secretagogues and bile acids on mitochondrial membrane potential of pancreatic acinar cells: comparison of different modes of evaluating DeltaPsim. J Biol Chem 2004;279:27327-38.
11. Mareninova OA, Hermann K, French SW, et al. Impaired autophagic flux mediates acinar cell vacuole formation and trypsinogen activation in rodent models of acute pancreatitis. J Clin Invest 2009;119:3340-55.
12. **Mareninova OA, Sendler M**, Malla SR, et al. Lysosome associated membrane proteins maintain pancreatic acinar cell homeostasis: LAMP-2 deficient mice develop pancreatitis. Cell Mol Gastroenterol Hepatol 2015;1:678-694.
13. Giorgio V, Bisetto E, Soriano ME, et al. Cyclophilin D modulates mitochondrial F0F1-ATP synthase by interacting with the lateral stalk of the complex. J Biol Chem 2009;284:33982-8.
14. Jones JW, Tudor G, Bennett A, et al. Development and validation of a LC-MS/MS assay for quantitation of plasma citrulline for application to animal models of the acute radiation syndrome across multiple species. Anal Bioanal Chem 2014;406:4663-75.
15. Gukovskaya A, Pandol S. Nitric oxide production regulates cGMP formation and calcium influx in pancreatic acinar cells. Am J Physiol 1994;266:G350-6.

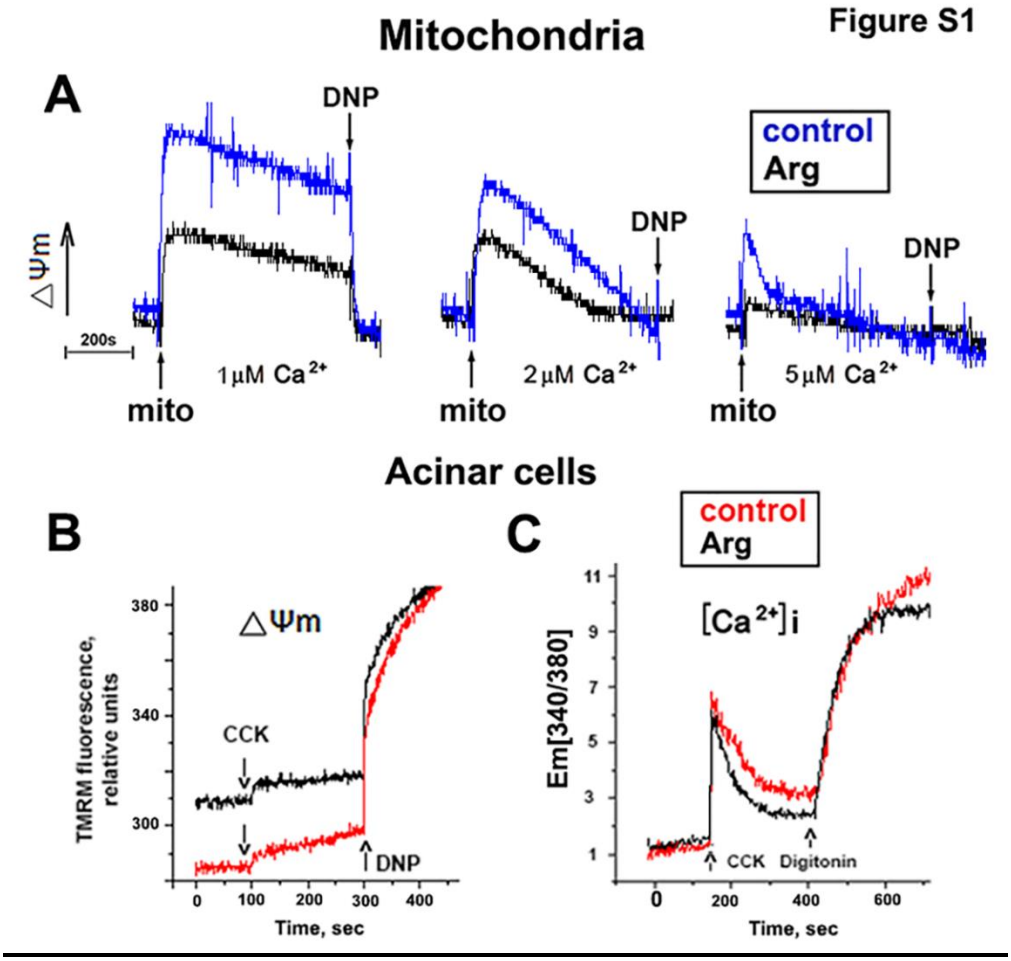

<u>Figure S1</u>. Mechanism of mitochondrial depolarization in Arg-AP differs from that induced by Ca^{2+} overload. (*A*). Wt mice were subjected to Arg-AP and killed after 24 h. Pancreatic mitochondria were isolated in the presence of 1 mM EGTA from control (saline-treated) and pancreatitic mice, and subjected to the indicated concentrations of free Ca^{2+} maintained with Ca^{2+}/EGTA buffers. Mitochondrial membrane potential ($\Delta\Psi m$) was measured with a tetraphenyl phosphonium ion (TPP^+) electrode. Arrows indicate additions of mitochondria suspension (mito) and 5 μM dinitrophenol (DNP; a mitochondrial uncoupler). Quantification of the effect of Ca^{2+} on $\Delta\Psi m$, based on these experiments, is presented in Figure 1*E*. (*B,C*). Isolated mouse pancreatic acinar cells were incubated for 3 h with and without 40 mM Arg, and then stimulated with 100 nM cholecystokinin-8 (CCK). Changes in $\Delta\Psi m$ (*B*) and $[Ca^{2+}]i$ (*C*) were measured in cell suspensions loaded with the $\Delta\Psi m$- or $[Ca^{2+}]i$-sensitive fluorescent probes TMRM and Fura-2, respectively. Changes in $[Ca^{2+}]i$ are expressed as the ratio of Fura-2 fluorescence intensity at 510 nm upon excitation at 340 and 380 nm. Digitonin was added at the end of the experiment to obtain maximal intensity of Fura-2 saturated with Ca^{2+}. Data are representative of at least 3 experiments on different acinar cell preparations.

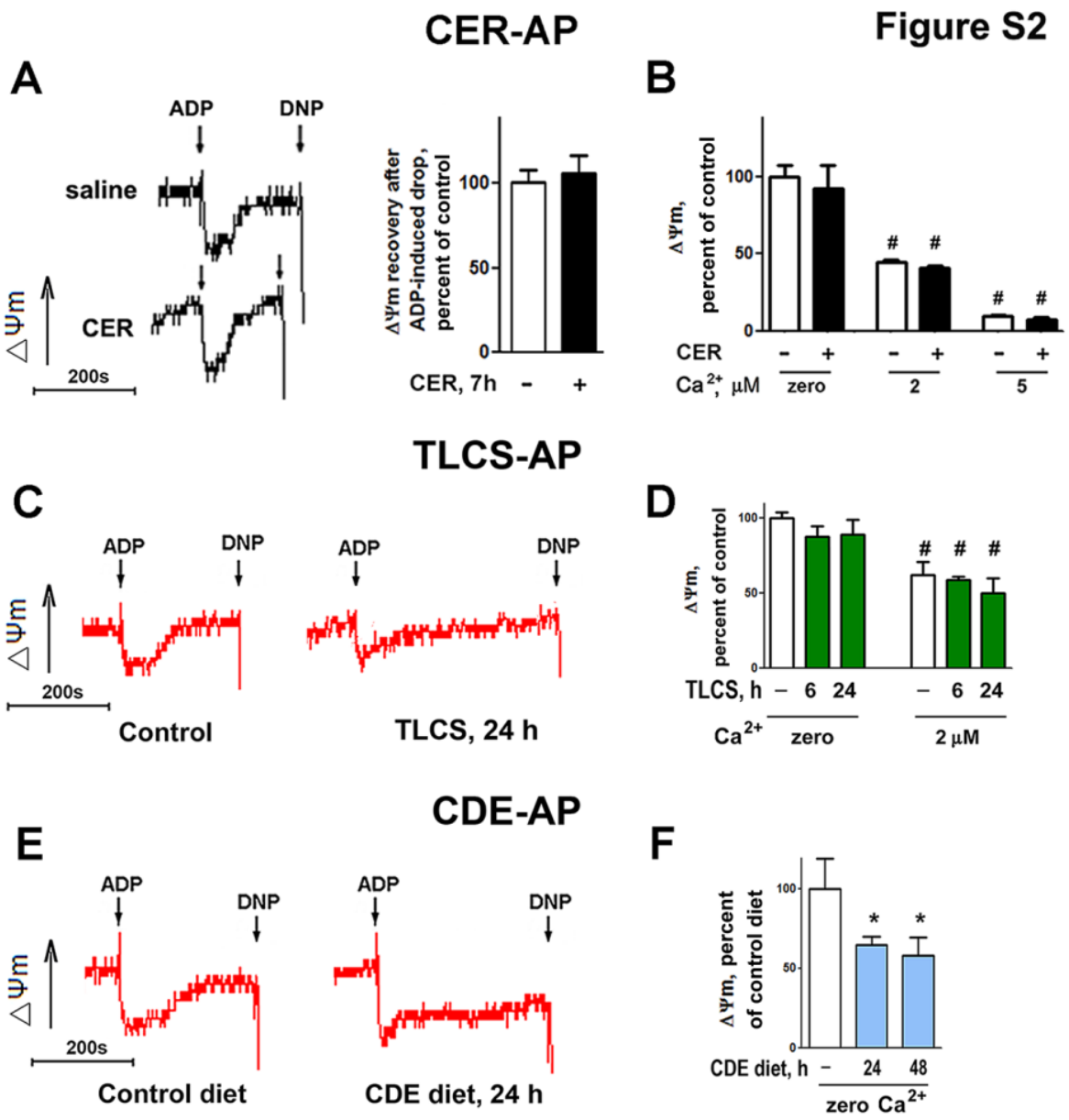

Figure S2. Characteristics of mitochondrial dysfunction in CER-AP, TLCS-AP, and CDE-AP. Mice were subjected to CER-AP (*A,B*), TLCS-AP (*C,D*) or CDE-AP (*E,F*), as detailed in *Methods*, and killed at indicated times. Pancreatic mitochondria were isolated and assayed either in Ca^{2+}-free medium containing 1 mM EGTA (*A,C,E,F*) or at indicated free Ca^{2+} concentrations maintained with Ca^{2+}/EGTA buffers (*B,D*). ΔΨm was measured with tetraphenyl phosphonium ion (TPP^+) electrode and quantified as in Figure 1. Arrows indicate additions of 20 μM ADP and 5 μM dinitrophenol (DNP; a mitochondrial uncoupler). Values are mean ± SEM from 3-5 mice for each condition. *p<0.05 versus mitochondria isolated from control mice; #p<0.05 versus mitochondria isolated from mice with the same treatment, but assayed at zero Ca^{2+}.

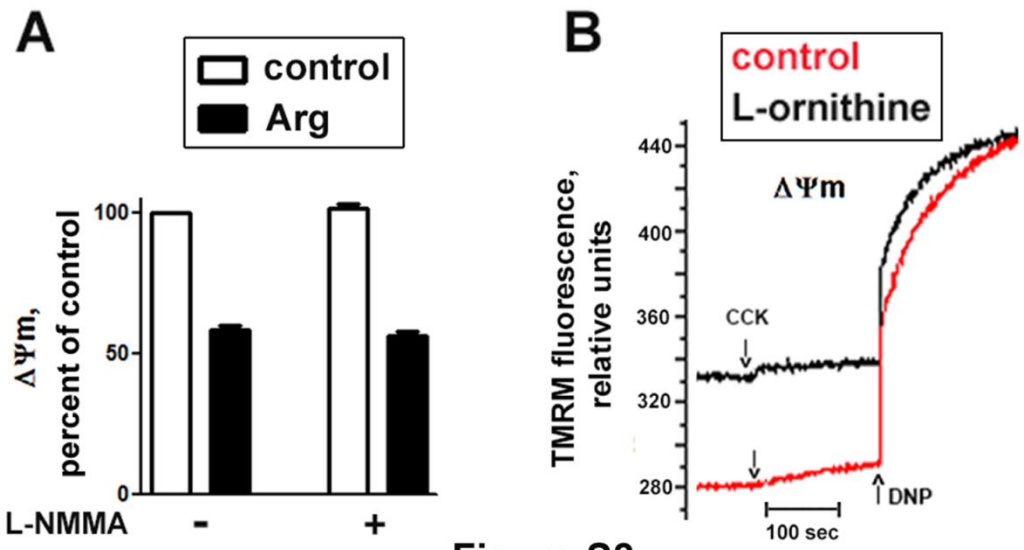

Figure S3

<u>Figure S3</u>. L-ornithine, but not NO synthase, mediates the effects of L-Arginine on ΔΨm. Isolated mouse pancreatic acinar cells were incubated for 3 h with and without 40 mM Arg (*A*) or L-ornithine (*B*). In (*A*), incubation was in the presence or absence of 1 mM L-NMMA, the dose that blocks NO synthase activity in acinar cells.[15] In (*B*), cells pre-incubated with or without L-ornithine were then stimulated with 100 nM cholecystokinin-8 (CCK). Changes in ΔΨm were measured in cell suspensions loaded with the ΔΨm-sensitive fluorescent probe TMRM; dinitrophenol (DNP; 5 μM) was added at the end of the experiment to dissipate ΔΨm. The data are representative of 3 experiments on different acinar cell preparations.

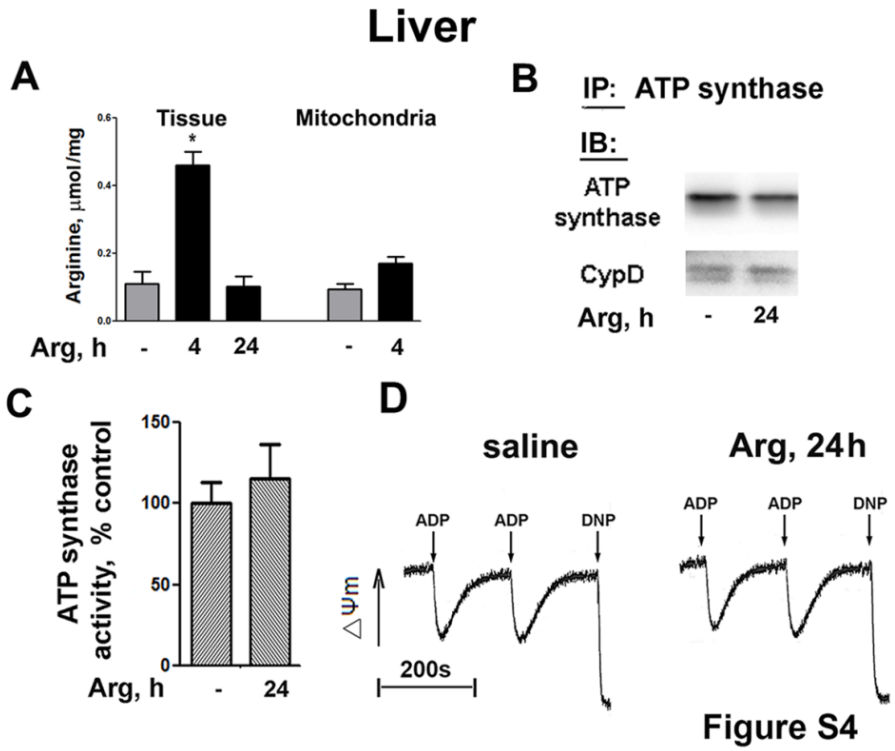

Figure S4

Figure S4. Liver mitochondria are not damaged in Arg-AP. Wt mice were subjected to Arg-AP, killed at indicated times, and liver tissue (*A*) and isolated liver mitochondria (*A-D*) were analyzed. (*A*). The levels of free Arg in homogenates of liver tissue and isolated liver mitochondria were measured with LC-MS and expressed per mg protein. (*B*). F-ATP synthase was immunoprecipitated (IP) from liver mitochondria isolated from mice at indicated conditions, and the levels of F-ATP synthase and CypD in the immunoprecipitates were measured by IB. (*C*). F-ATP synthase enzymatic activity was measured as in Figure 2*B,C* and normalized to that in control (saline-treated) mice. (*D*). Changes in $\Delta\Psi m$ were recorded with a tetraphenyl phosphonium ion (TPP^+) electrode; arrows indicate additions of 20 µM ADP and 5 µM DNP (mitochondrial uncoupler). Values in (*A*) and (*C*) are mean ± SEM from at least 3 mice for each condition. *p< 0.05 versus control (saline-treated) mice.

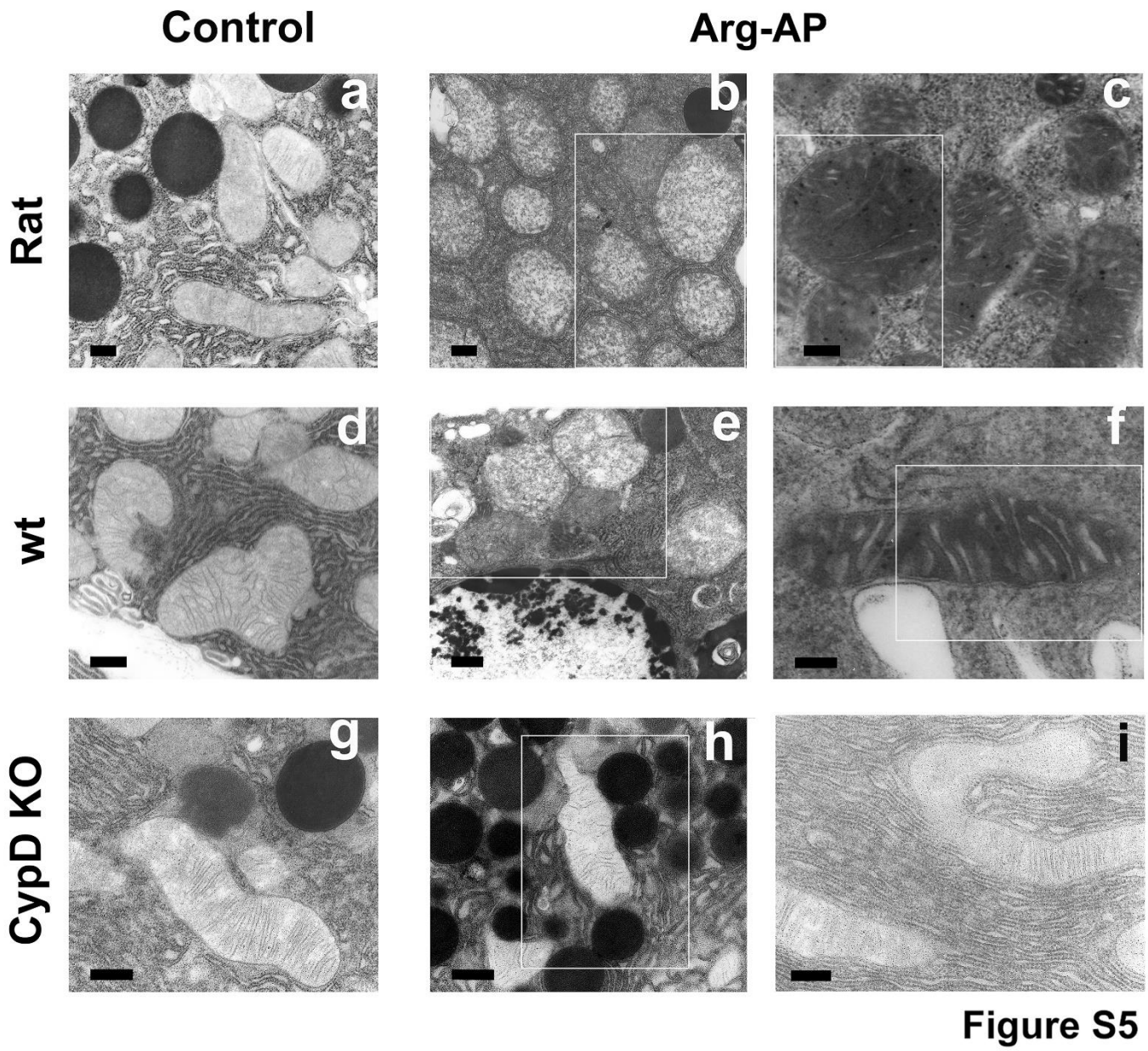

Figure S5

Figure S5. CypD genetic ablation prevents pathologic ultrastructural alterations in pancreatic mitochondria caused by Arg-AP. Rats (a-c), and wt (d-f) and CypD KO (g-i) mice were subjected to Arg-AP, killed at 2 h (b), 4 h (a, c) or 24 h (d-i), and pancreatic tissue was analyzed. EM shows mitochondria with loss of cristae and flocculent matrix (b, e); or condensed matrix and dilated cristae (c, f) in pancreas of rats and wt mice with Arg-AP. The pathologic alterations in mitochondrial ultrastructure in Arg-AP were essentially prevented by CypD genetic ablation. Scale bar: 0.5 µm. Boxed areas are those presented in Figure 2*H*.

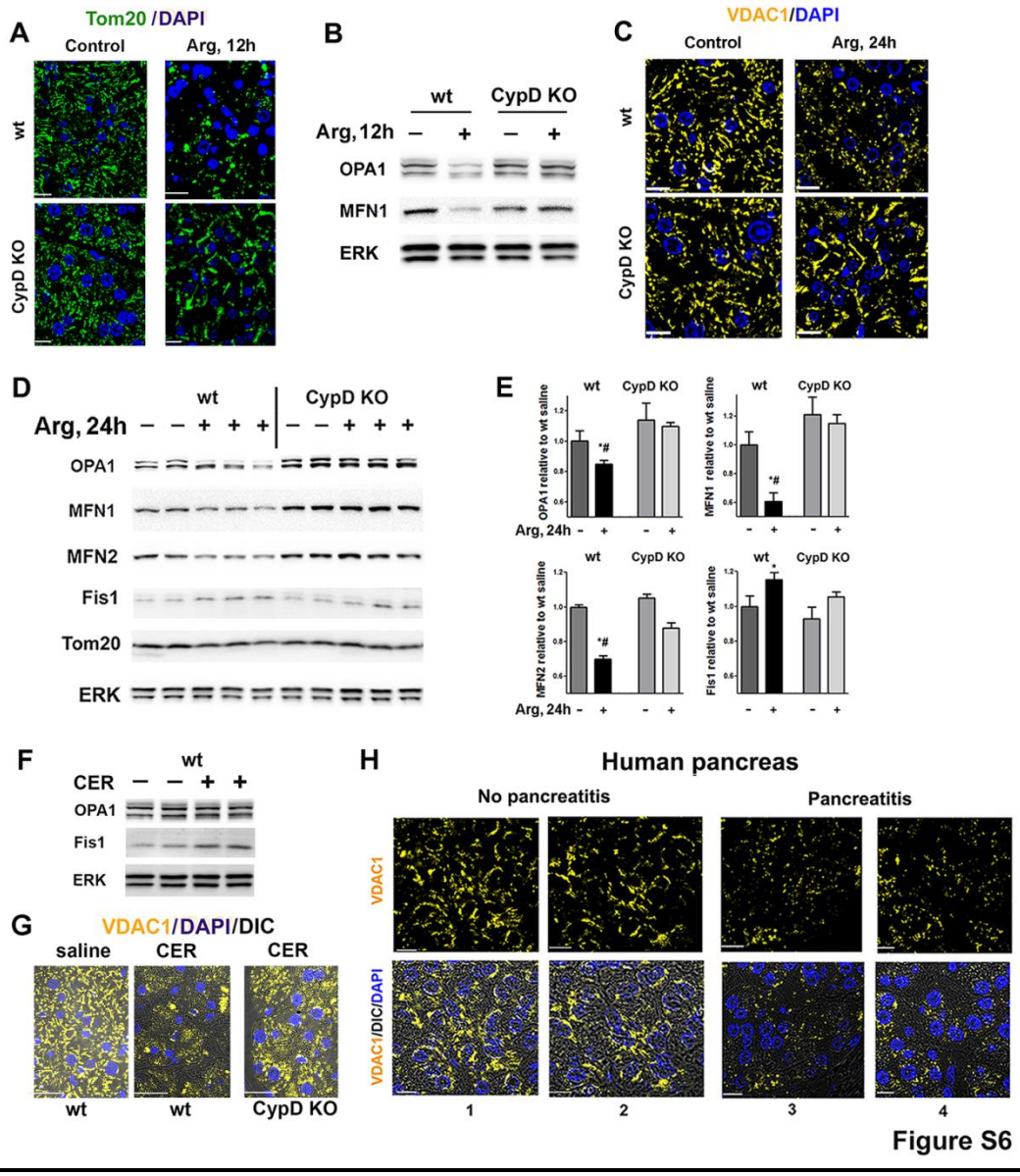

Figure S6

<u>Figure S6</u>. Arg-AP and CER-AP cause mitochondrial fragmentation, which is prevented by CypD genetic ablation. Mitochondrial fragmentation is prominent in human pancreatitis. Parameters of mitochondrial dynamics were measured in pancreas of wt and CypD KO mice subjected to Arg-AP (*A,B*: 12 h; *C-E*: 24 h) or CER-AP (*F,G*); and in human normal pancreas and pancreatitis (*H*). Pancreatic tissue sections were immunostained for the mitochondrial markers Tom20 (*A*) or VDAC1 (*C,G,H*) and visualized with confocal microscopy. Nuclei were stained with DAPI; differential interference contrast (DIC) was used to display zymogen granules area in acinar cells. Each tissue section in (*H*) is from a different patient; images #1 and 2 represent normal pancreas, and #3 and 4, pancreatitis tissue (from a total of 21 patients). Scale bars: 10 µm (*A* and *H*) and 25 µm (*G*). (*B,D-F*). Protein levels of markers of mitochondrial fusion (OPA1, MFN1, MFN2) and fission (Fis1), and the mitochondria resident (import receptor) Tom20 were measured by IB. In this and other figures, ERK1/2 or GAPDH are loading controls, and each lane represents an individual animal. (*E*). For every protein shown in (*D*), densitometric band intensities were normalized to that of ERK in the same sample, and the mean ratios further normalized to that in wt control group. Values are mean ± SEM (n=3 per group). *p<0.05 versus wt control (saline-treated) mice; #p<0.05 versus CypD KO mice with Arg-AP.

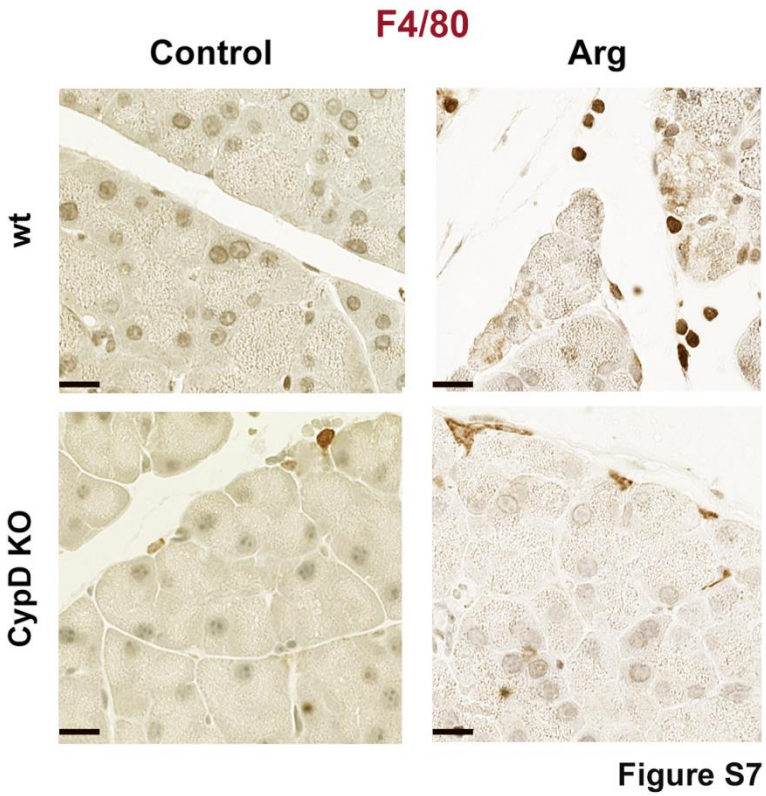

Figure S7

Figure S7. CypD genetic ablation reduces macrophage infiltration in Arg-AP. IHC for the macrophage marker F4/80 on pancreatic tissue sections from wt and CypD KO mice that were subjected to Arg-AP and killed 24 h later. Scale bar: 10 µm. Quantification of the F4/80 immunostaining is presented in Figure 4*D*.

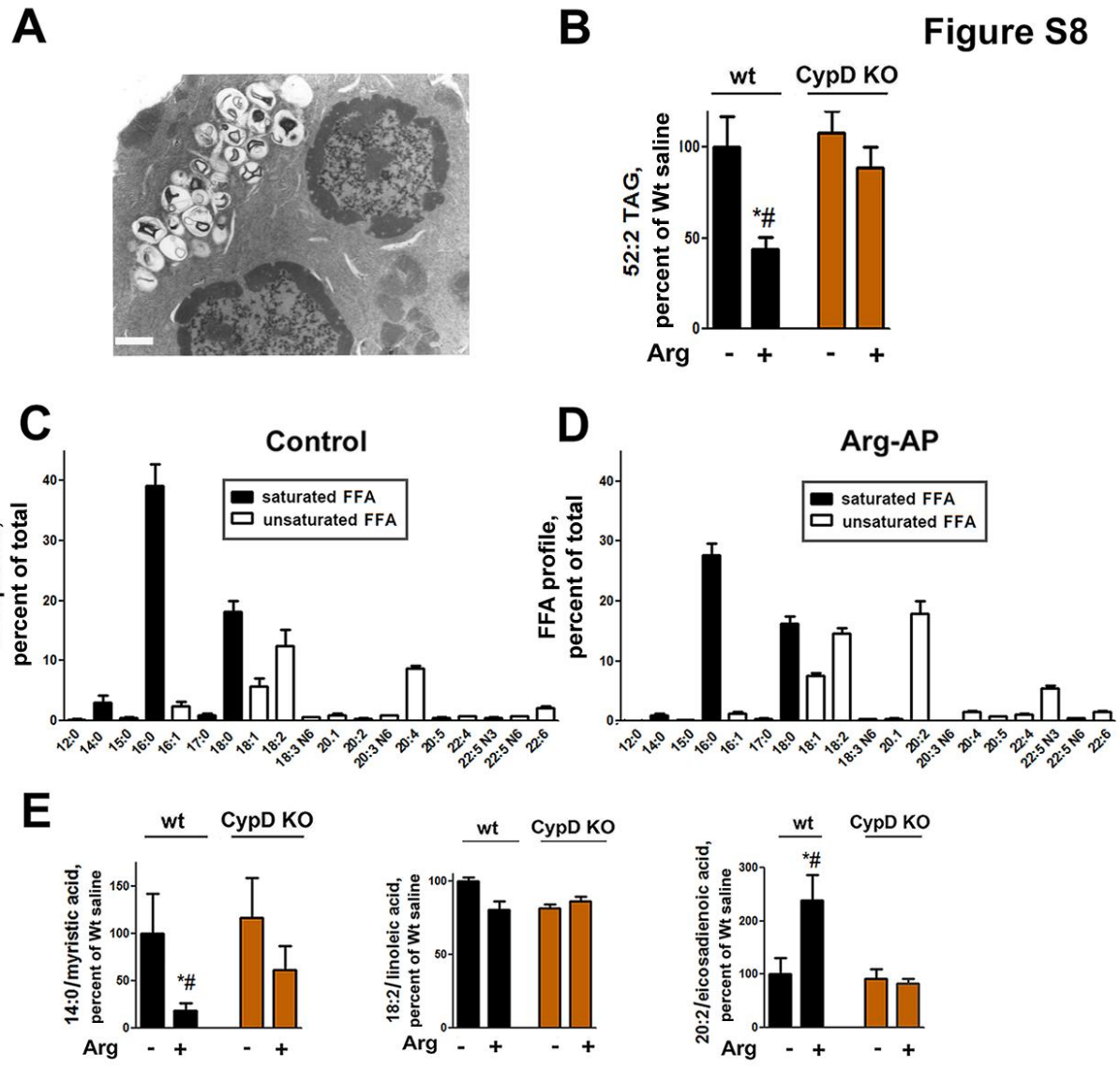

Figure S8. Alterations in lipid metabolism in Arg-AP. Rats (*A*) and mice (*B-E*) were subjected to 24 h Arg-AP. (*A*). EM showing accumulation of lamellar bodies in pancreatic acinar cells of rats with Arg-AP. Scale bar: 2.5 µm. (*B–E*). Changes in pancreatic lipid metabolism were analyzed with LC-MS and GC-MS as detailed in *Methods*. (*B, E*). The levels of indicated TAGs and FFAs in pancreatic tissue, expressed per mg protein and normalized to those in wt control (saline treated) mice. (*C, D*). Pancreatic FFA profiles expressed as percent of total. For each FFA and TAG, the number of carbons/number of double bonds is shown. Values are mean ± SEM from 3 mice per group. *p<0.05 versus wt control (saline treated) mice; $^{\#}$p<0.05 versus the same treatment in CypD KO mice.

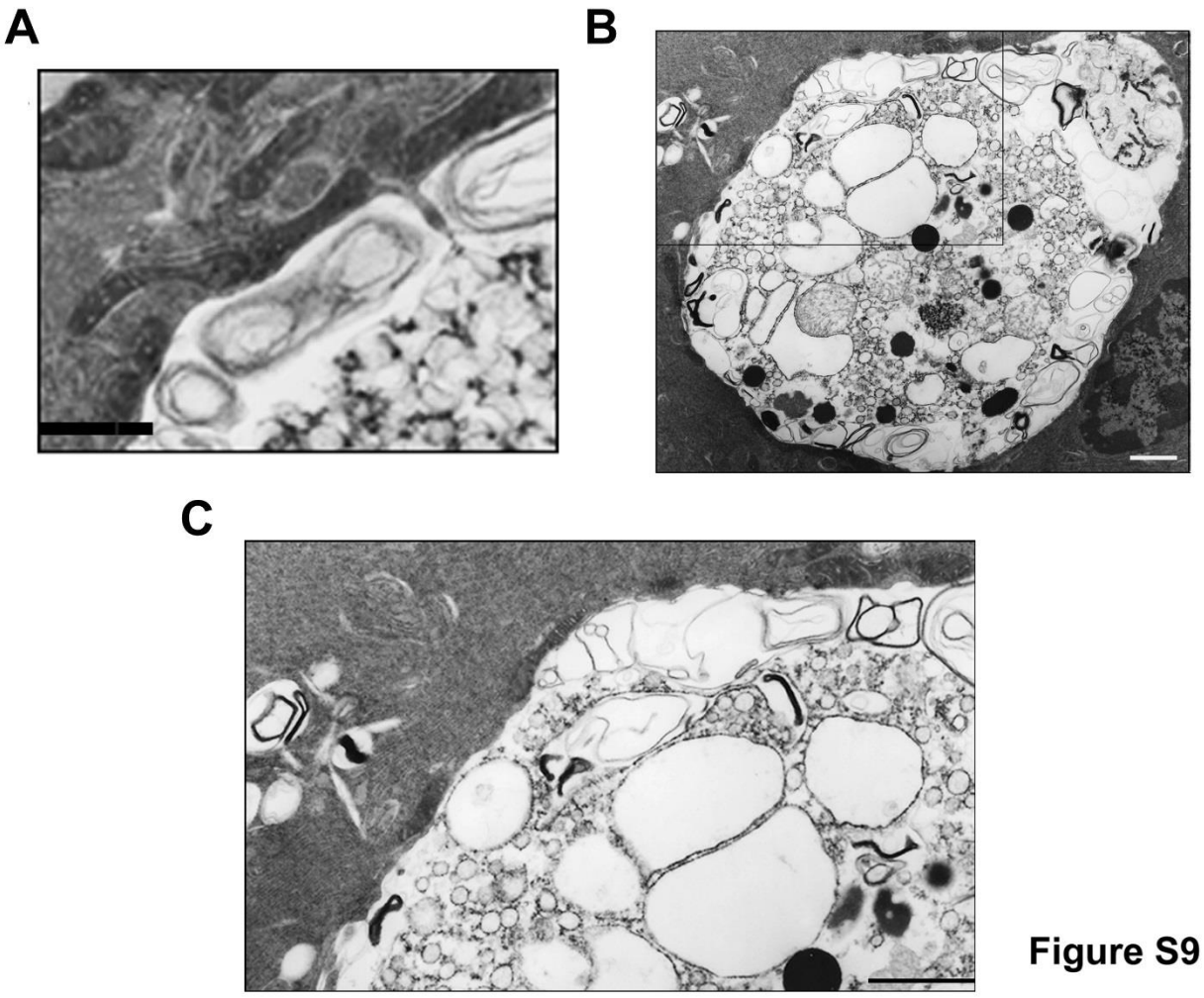

Figure S9. Juxtaposition of condensed mitochondria and abnormally large autolysosomes in pancreas of mice with Arg-AP. (*A*). Enlarged area of the electron micrograph shown boxed in Figure 5*C*. (*B*). Abnormally large autolysosome containing poorly degraded zymogen granules, mitochondria, and lipid inclusions. (*C*). Enlarged boxed area of (*B*) showing autolysosomes "wrapped" with condensed mitochondria. Scale bars: 2 µm (*A*); 3 µm (*B, C*).

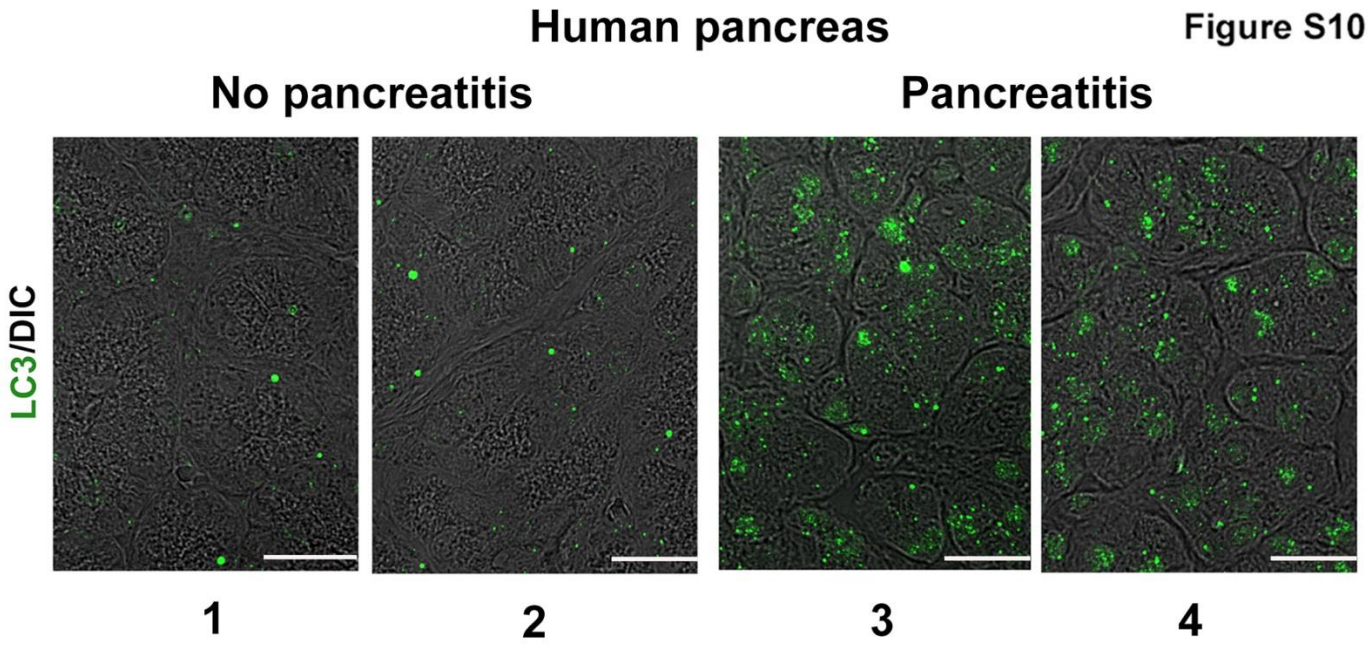

Figure S10. Accumulation of autophagic vacuoles in human pancreatitis. Human pancreatic tissue sections were immunostained for LC3, a marker of autophagic vacuoles, and the LC3-positive puncta visualized with confocal microscopy. Differential interference contrast (DIC) was used to display zymogen granules area in acinar cells. Each tissue section is from a different patient; images #1 and #2 represent normal pancreas, and #3 and #4, pancreatitis tissue (from a total of 21 patients). Scale bar: 20 μm.

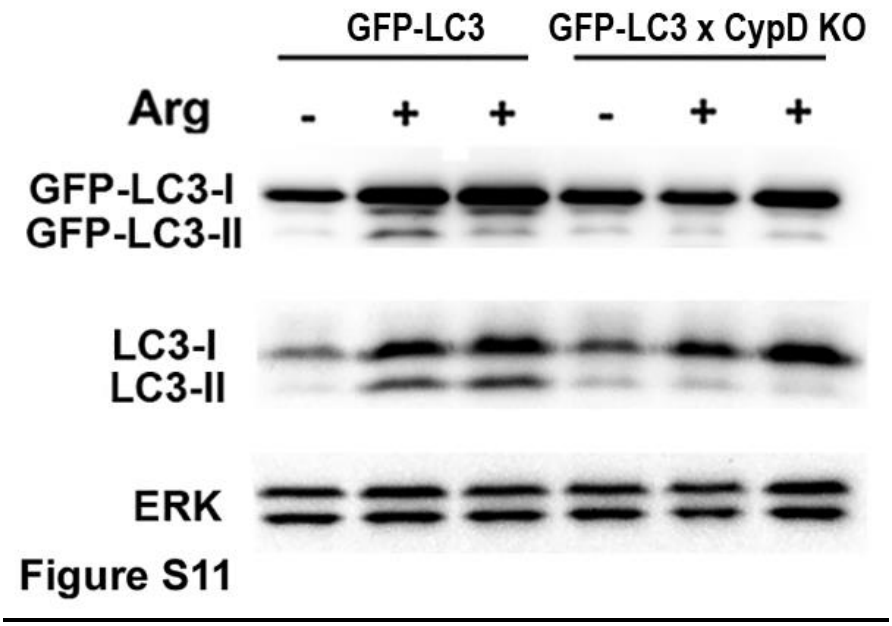

Figure S11. CypD genetic ablation normalizes autophagy in GFP-LC3 transgenic mice subjected to Arg-AP. GFP-LC3 mice and GFP-LC3;CypD KO compound mice were subjected to Arg-AP, killed 24 h later, and pancreatic levels of both GFP-LC3 and endogenous LC3 were measured by IB.

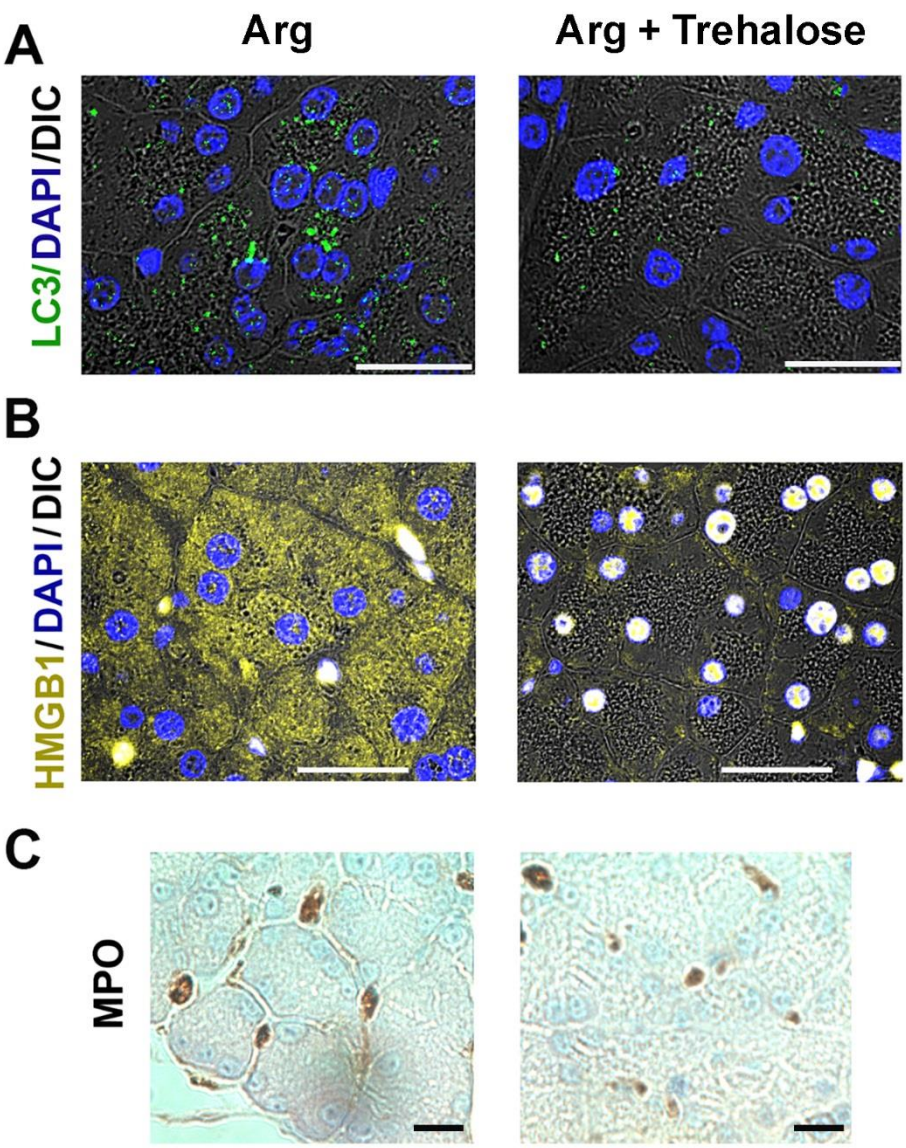

Figure S12

Figure S12. Enhancement of autophagic activity with trehalose improves Arg-AP. Wt mice received daily i.p. injections of trehalose (or vehicle) for 2 weeks, then subjected to Arg-AP, killed 24 h later, and pancreatic tissue was analyzed. (*A, B*). IF analysis of LC3 (green) and HMGB1 (yellow) in pancreas. Nuclei were stained with DAPI (blue); differential interference contrast (DIC) was used to display zymogen granules area in acinar cells. Note massive release of HMGB1 from nuclei in Arg-AP, which is completely prevented with trehalose (nuclei colored white from merged HGMB1 and DAPI). (*C*). Infiltrating neutrophils were detected on pancreatic tissue sections with IHC for myeloperoxidase (MPO). Scale bars: 20 µm (*A, B*); 10 µm (*C*). Quantification of the immunostaining for MPO and HMGB1 is presented in Figures 3 and 6.

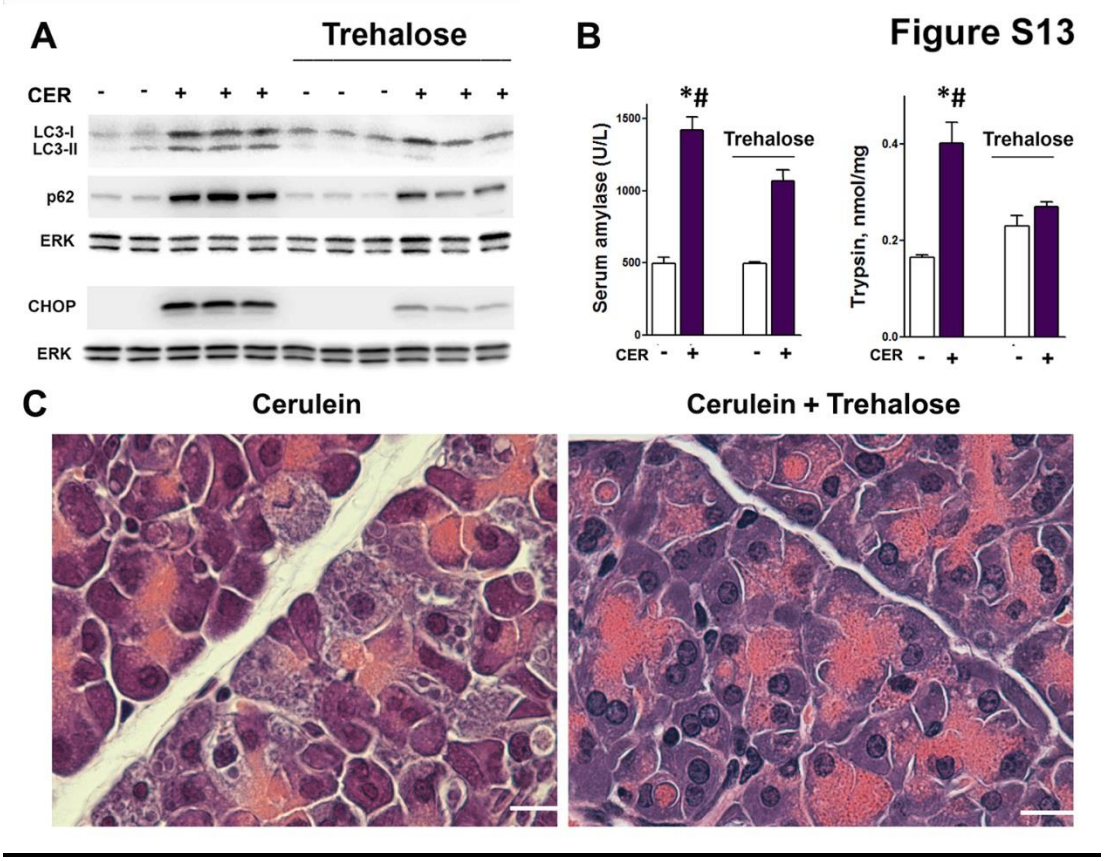

Figure S13. Enhancement of autophagic activity with trehalose improves CER-AP. Wt mice received daily i.p. injections of trehalose (or vehicle) for 2 weeks, then subjected to 7 h CER-AP, and pancreatic tissue was analyzed. (*A*). IB analysis for the markers of autophagy (LC3-I/II and p62) and ER stress (CHOP). (*B, C*). Serum amylase, trypsin activity, and histopathologic changes were assessed as in Figure 3. Values are mean ± SEM from 4 mice for each condition.

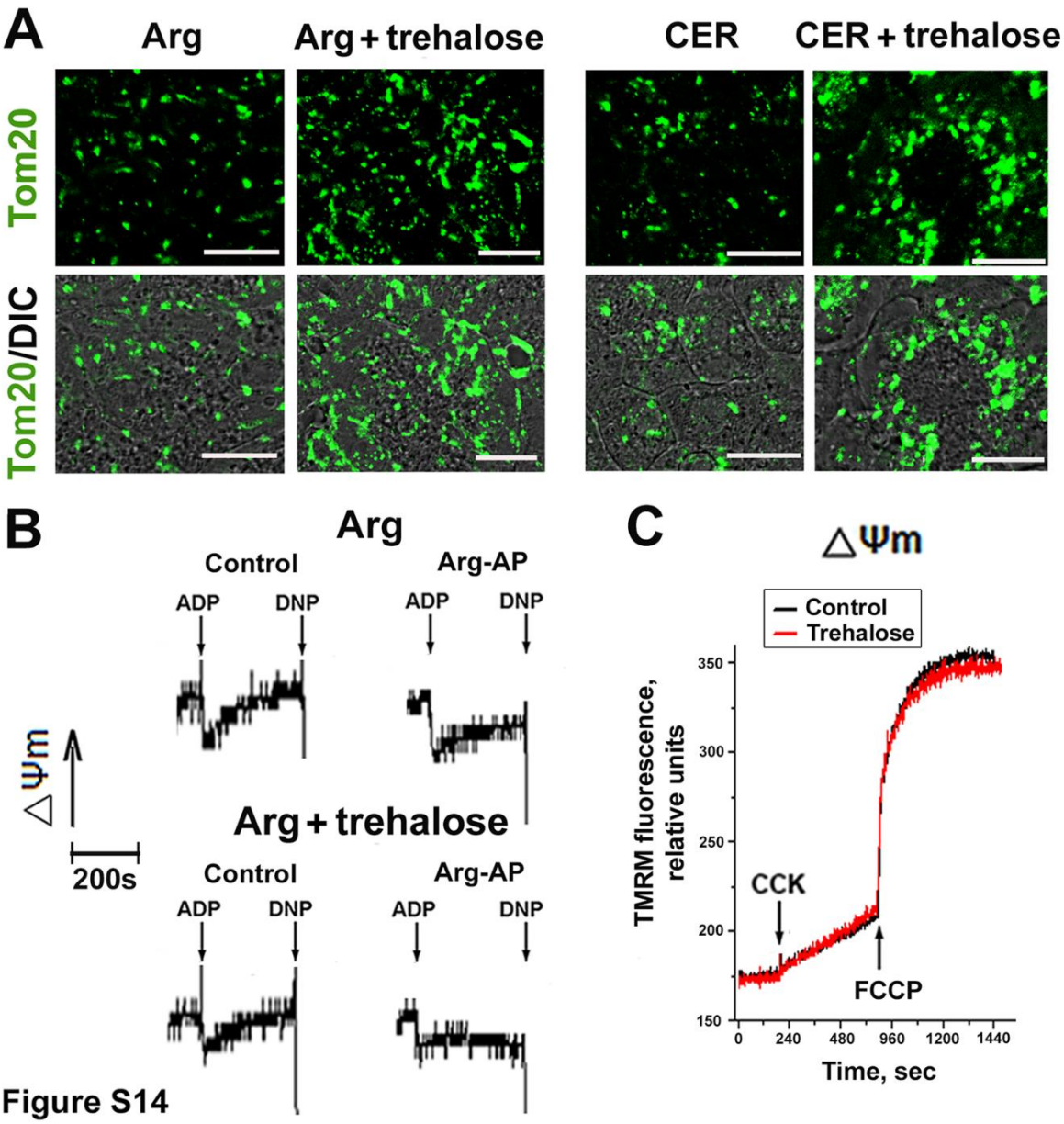

Figure S14

<u>Figure S14</u>. Trehalose has no direct effect on pancreatic mitochondria. Wt mice received daily i.p. injections of trehalose (or vehicle) for 2 weeks, then subjected to 24 h Arg-AP or 7 h CER-AP. (*A*). Pancreatic tissue sections were immunostained for the mitochondrial marker Tom20 and visualized with confocal microscopy. Differential interference contrast (DIC) was used to display zymogen granules area in acinar cells. Scale bars: 10 µm. (*B*). Pancreatic mitochondria were isolated and assayed in Ca^{2+}-free medium containing 1 mM EGTA. ΔΨm was measured in mitochondrial suspension with tetraphenyl phosphonium ion (TPP^{+}) electrode. Arrows indicate additions of 20 µM ADP and 5 µM DNP (mitochondrial uncoupler). (*C*). Isolated mouse pancreatic acinar cells were incubated for 2 h with and without 100 mM trehalose, and then stimulated with 100 nM CCK. Changes in ΔΨm were measured in cell suspension loaded with the ΔΨm-sensitive fluorescent probe TMRM. 10 µM FCCP (mitochondrial uncoupler) was added in the end of each experiment to dissipate ΔΨm. The data are representative of 3 experiments on different mitochondria or cell preparations.

Table 1. Parameters of pancreatic mitochondria dysfunction differ between mouse AP models.

Pancreatitis model, time after induction	Mitochondria from mice with pancreatitis were isolated and assayed in a Ca^{2+} free medium containing EGTA		Acinar cells incubated with pancreatitis toxins in standard medium (containing 1 mM Ca^{2+})			Effect of CypD genetic ablation on pancreatitis responses
	Loss of $\Delta\Psi m$	$\Delta\Psi m$ recovery after ADP-induced drop	Toxin	Loss of $\Delta\Psi m$	BAPTA prevents $\Delta\Psi m$ loss	
Arg-AP, 24 h	Yes	No	Arg	Yes	No	Improves (this study)
CDE-AP, 24 h	Yes	No	–	–	–	Improves (Ref. 4)
CER-AP, 7 h	No	Yes	CCK-8	Yes	Yes	Improves (this study and Ref. 4)
TLCS-AP, 24 h	No	Yes	TLCS	Yes	Yes	Improves (Ref. 4)